

JPL Publication 91-36

NASA
1N-44-CR
46779
P. 24

Results of the 1991 NASA/JPL Balloon Flight Solar Cell Calibration Program

B. E. Anspaugh
R. S. Weiss

(NASA-CR-188968) RESULTS OF THE 1991
NASA/JPL BALLOON FLIGHT SOLAR CELL
CALIBRATION PROGRAM (JPL) 24 p CSCL 10A

N92-12332

G3/44 Unclass
0046779

October 1, 1991

NASA

National Aeronautics and
Space Administration

Jet Propulsion Laboratory
California Institute of Technology
Pasadena, California



JPL Publication 91-36

Results of the 1991 NASA/JPL Balloon Flight Solar Cell Calibration Program

B. E. Anspaugh
R. S. Weiss

October 1, 1991

NASA

National Aeronautics and
Space Administration

Jet Propulsion Laboratory
California Institute of Technology
Pasadena, California

The research described in this publication was carried out by the Jet Propulsion Laboratory, California Institute of Technology, under a contract with the National Aeronautics and Space Administration.

Reference herein to any specific commercial product, process, or service by trade name, trademark, manufacturer, or otherwise, does not constitute or imply its endorsement by the United States Government or the Jet Propulsion Laboratory, California Institute of Technology.

ABSTRACT

The 1991 solar cell calibration balloon flight was completed on August 1, 1991. All objectives of the flight program were met. Thirty-nine modules were carried to an altitude of 119,000 ft (36.3 km). Data telemetered from the modules were corrected to 28°C and to 1 AU. The calibrated cells have been returned to the participants and can now be used as reference standards in simulator testing of cells and arrays.

ACKNOWLEDGMENT

The authors wish to express appreciation for the cooperation and support provided by the entire staff of the National Scientific Balloon Facility located in Palestine, Texas. The cooperation and patience extended by all participating organizations are greatly appreciated.

CONTENTS

1. INTRODUCTION AND OVERVIEW	1
2. PREFLIGHT PROCEDURES	1
2.1 MODULE FABRICATION	1
2.2 CELL MEASUREMENTS	1
2.3 TEMPERATURE COEFFICIENTS AND LEAST SQUARES FITS	2
2.4 PANEL ASSEMBLY AND CHECKOUT	2
2.5 PRELAUNCH PROCEDURES AT PALESTINE	2
3. BALLOON SYSTEM	6
3.1 BALLOON DESCRIPTION	6
3.2 TOP PAYLOAD	6
3.3 BOTTOM PAYLOAD	7
4. FLIGHT SEQUENCE	9
4.1 PRELAUNCH PREPARATIONS	9
4.2 FLIGHT	12
4.3 FLIGHT TERMINATION	12
5. DATA ANALYSIS	14
5.1 COMPUTER ANALYSIS	14
5.2 CALIBRATION RESULTS	15
5.3 DATA REPEATABILITY	15
6. CONCLUSIONS	15
7. REFERENCE	15

Figures

Figure 1. Photograph of the 1991 Balloon Flight Solar Panel	3
Figure 2. 1991 Module Location Chart	4
Figure 3. Aluminum Hoop Assembly With Tracker Mounted	5
Figure 4. Block Diagram of Balloon Telemetry System	8
Figure 5. Flight Train Configuration	10
Figure 6. Balloon Launch	11
Figure 7. 1991 Balloon Launch Flight Profile	13

Tables

Table 1. 1991 Balloon Flight 8/1/91 119,000 ft, RV = 1.0149684, Flight No. 1504P	16
Table 2. Repeatability of Eight Standard Solar Cell Modules Over an 11-year Period	17

1. INTRODUCTION AND OVERVIEW

The primary source of electrical power for unmanned space vehicles is the direct conversion of solar energy through the use of solar cells. As advancing cell technology continues to modify the spectral response of solar cells to utilize more of the sun's spectrum, designers of solar cells and arrays must have the capability of measuring these cells in a light beam that is a close match to the solar spectrum. The solar spectrum has been matched very closely by laboratory solar simulators. But the design of solar cells and the sizing of solar arrays require such highly accurate measurements that the intensity of these simulators must be set very accurately. A small error in setting the simulator intensity can conceivably cause a disastrous missizing of a solar panel, causing either a premature shortfall in power or the launch of an oversized, overweight solar panel.

The Jet Propulsion Laboratory (JPL) solar cell calibration program was conceived to produce reference standards for the purpose of accurately setting solar simulator intensities. The concept was to fly solar cells on a high-altitude balloon, measure their output at altitudes near 120,000 ft, recover the cells, and use them as reference standards. The procedure is simple. The reference cell is placed in the simulator beam, and the beam intensity is adjusted until the reference cell reads the same as it read on the balloon. As long as the reference cell has the same spectral response as the cells or panels to be measured, this is a very accurate method of setting the intensity. But as solar cell technology changes, the spectral response of the solar cells changes also, and reference standards using the new technology must be built and calibrated.

Until the summer of 1985, there had always been a question as to how much the atmosphere above the balloon modified the solar spectrum. If the modification were significant, the reference cells might not have the required accuracy. Solar cells made in recent years have increasingly higher blue responses, and if the atmosphere has any effect at all, it would be expected to modify the calibration of these newer blue cells much more so than for cells made in the past.

In late 1984, a collection of solar cells representing a wide cross section of solar cell technology was flown on the shuttle Discovery as a part of the Solar Cell Calibration Facility (SCCF) experiment. The cells were calibrated as reference cells on this flight by using procedures similar to those used on the balloon flights. The same cells were then flown on the 1985 balloon flight and remeasured. Since the

two sets of measurements gave nearly identical results (see the reference), the reference standards from balloon flights may continue to be used with high confidence.

JPL has been flying calibration standards on high-altitude balloons since 1963 and continues to organize a calibration balloon flight at least once a year. The tradition was continued this year with the 1991 flight, which incorporated 39 solar cell modules from 9 different participants. Two of the modules had two cells mounted, so there was a total of 41 calibration cells flown. The cells included Si, GaAs, GaInP and CuInSe₂ cells from both domestic and foreign manufacturers.

2. PREFLIGHT PROCEDURES

2.1 MODULE FABRICATION

The cells were mounted by the participants or by JPL on JPL-supplied standard modules according to standard procedures developed for the construction of reference cells. The JPL standard module is a machined copper block on which a fiberglass circuit board is mounted. The circuit board has insulated solder posts which are used for making electrical connections to the solar cell and to a load resistor. This assembly is painted with either high-reflectance white or low-reflectance black paint. The resistor performs two tasks. First, it loads the cells near short-circuit current, which is the cell parameter that varies in direct proportion to light intensity. Second, it scales the cell outputs to read near 100 mV during the flight, which matches a constraint imposed by the telemetry electronics. Load resistance values are 0.5 ohm for a 2 x 2 cm cell, 0.25 ohm for a 2 x 4 cm cell, etc. The load resistors are precision resistors (0.1 percent, 20 ppm/°C) and have a resistance stability equal to or better than $\pm 0.002\%$ over a three-year period. The solar cells are permanently glued to the body of the machined copper block with RTV 560 or its equivalent. This gives a good thermal conductivity path between cell and copper block, while providing electrical insulation between the rear surface of the solar cells and the block.

2.2 CELL MEASUREMENTS

After the cells were mounted on the copper blocks, the electrical output of each cell module was measured under illumination by the JPL X25 Mark II solar simulator. For these measurements, the simulator intensity was set by using only one reference cell--no attempt was made to match the spectral response of the reference standard to the individual

cell modules. The absolute accuracy of these measurements is therefore unknown, but the measurements do allow checking of the modules for any unacceptable assembly losses or instabilities. After the balloon flight, the cells were measured in exactly the same way to check for any cell damage or instabilities that may have occurred as a result of the flight.

2.3 TEMPERATURE COEFFICIENTS AND LEAST SQUARES FITS

The temperature coefficients of the mounted cells were also measured before the flight. The modules were mounted in their flight configuration on a temperature controlled block in a vacuum chamber. Outputs were measured at 0, 20, 40, 60, and 80°C under illumination with the X25 simulator. The temperature coefficients of the cell modules were computed by fitting the output vs temperature relationship with a linear least squares fit.

2.4 PANEL ASSEMBLY AND CHECKOUT

After the electrical measurements were completed, the modules were mounted on the solar panel and connected electrically. Figure 1 is a photograph of the modules after completion of these steps, and Figure 2 is a diagram that identifies the modules in the photograph by their serial numbers. After completion of the panel assembly, the panel and tracker together were given complete functional tests in terrestrial sunlight. The assembled tracker and panel were placed in sunlight on a clear, bright day, and checked for the tracker's ability to acquire and track the sun while each cell module was checked for electrical output. When these tests were completed satisfactorily, the assembly was shipped to the National Scientific Balloon Facility (NSBF) in Palestine, Texas, for flight.

2.5 PRELAUNCH PROCEDURES AT PALESTINE

The NSBF was established in 1963 at Palestine, Texas. This location was chosen because it has favorable weather conditions for balloon launching and a large number of clear days with light surface winds. The high-altitude winds in this part of the country take the balloons over sparsely populated areas so the descending payloads are unlikely to cause damage to persons or property. The JPL calibration flights have flown from the Palestine facility since 1973. The flights are scheduled to fly in the June to September time period, since the sun is high in the sky at that time of year, and the sunlight passes through a minimum depth of atmosphere before reaching the solar modules.

Upon arrival at Palestine, the tracker and module payload were again checked for proper operation. This included a checkout in an environmental test chamber wherein the tracker, data encoder, and voltage reference box were all tested as a system. The chamber was pumped down to a pressure of ≈ 55 mb (corresponding to an altitude of 65,000 ft), cooled to -35°C, and the system was thoroughly tested. Then, the assembly was removed from the environmental chamber and a room-temperature, end-to-end check was performed on the payload, telemetry, receiving, and decoding systems. The four output voltage levels of the voltage reference box were wired into the telemetry stream along with the module outputs. The analog-to-digital converter system was calibrated by recording these four voltage levels as they were input to the system and as they were converted, decoded, and sent through the system as digital output values. The thermistor channels were calibrated by replacing each thermistor, in turn, with a known calibration resistor while the entire system was operating. Eleven resistors are used in this procedure to produce calibrations at 10 deg increments over the 0 to 100°C range. The checkout was completed by watching the system over a period of 2 to 3 hours to make sure that no stability problems occurred.

After all the checkouts and calibrations were performed, the tracker was mounted onto the aluminum tubular hoop assembly which will ride on the top portion (or apex) of the balloon. Figure 3 is a photograph of the hoop assembly with the tracker mounted.

ORIGINAL PAGE
BLACK AND WHITE PHOTOGRAPH

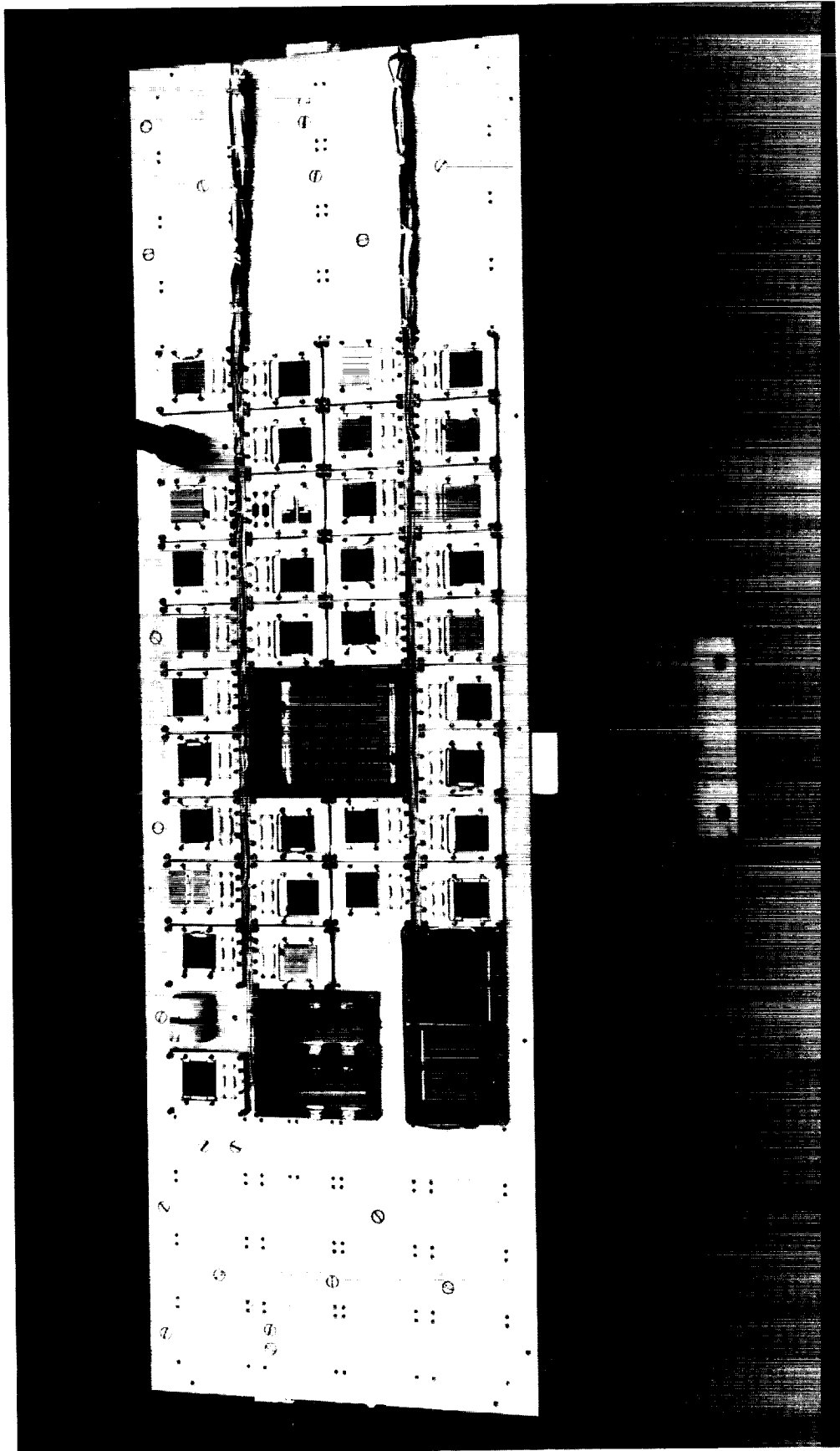
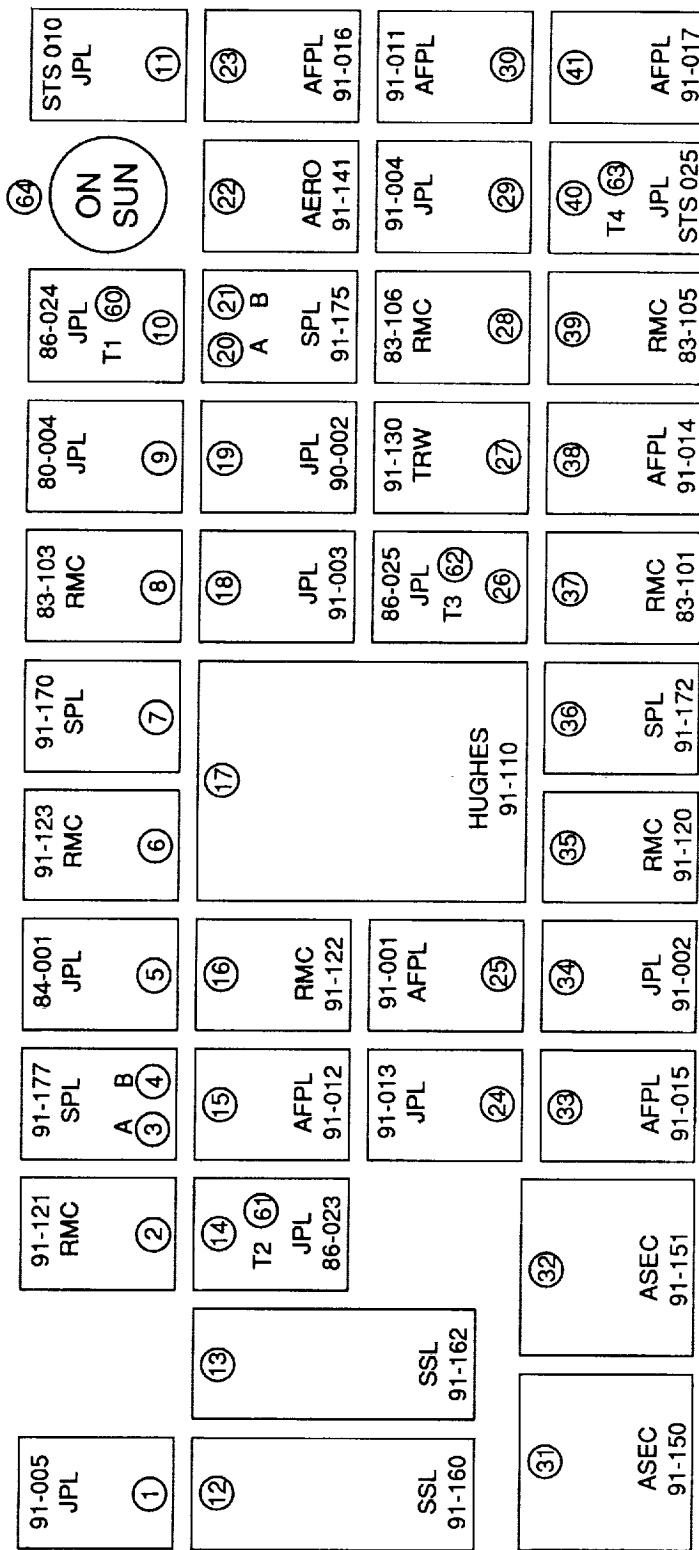


Figure 1. Photograph of the 1991 Balloon Flight Solar Panel



ORIGINAL PAGE
BLACK AND WHITE PHOTOGRAPH

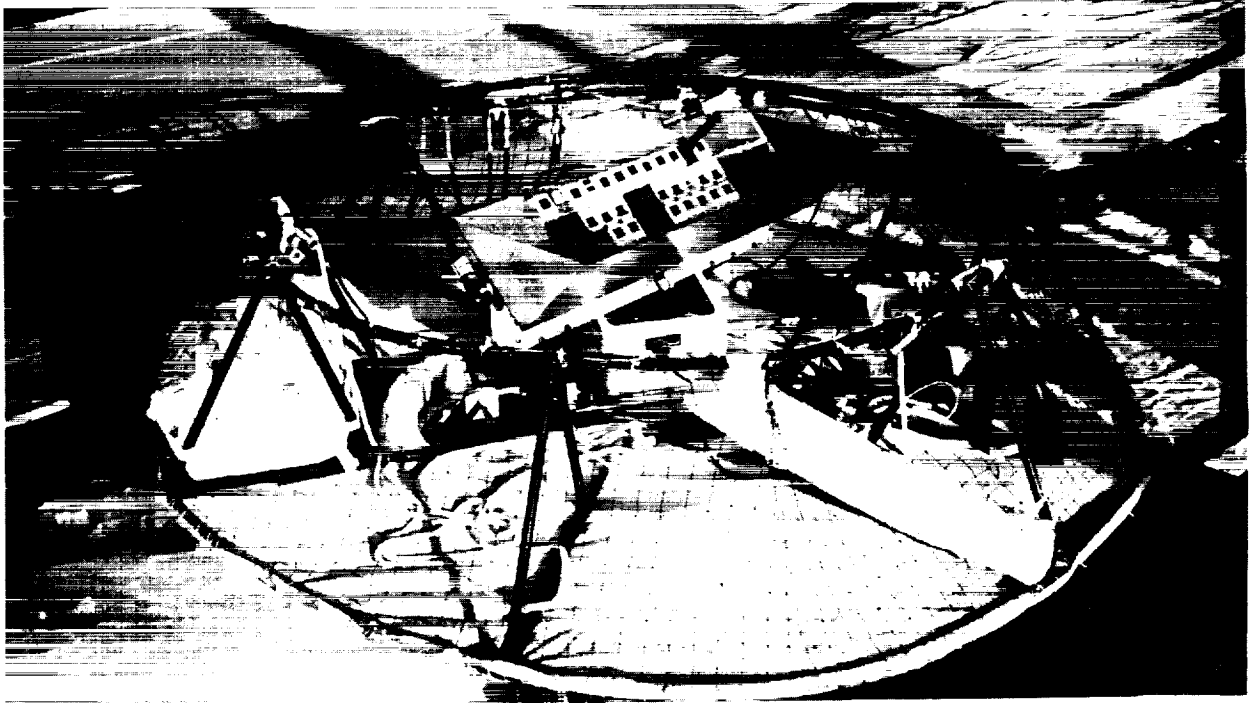


Figure 3. Aluminum Hoop Assembly With Tracker Mounted

3. BALLOON SYSTEM

The main components of the balloon flight system were (1) the apex-mounted hoop assembly that contains the experimental package, the data encoder, the recovery system, and the camera package; (2) the balloon; and (3) the lower payload that contains the telemetry and power systems.

3.1 BALLOON DESCRIPTION

The balloon used for the JPL solar cell calibration high-altitude flights had a volume of 3.49 million ft³ (99,000 m³) and was made from 0.8 mil (20 μm) stratofilm, a polyethylene film designed for balloon use. The balloon alone weighs 704 lb (319 kg). The balloon was designed to lift itself, along with the bottom and top payloads, to a float altitude of 120,000 ft (36 km). At float altitude, the balloon will have a diameter of roughly 188 ft (59 m). A multiconductor cable to electrically connect the top and bottom payloads was built into the balloon during its manufacture. The balloon was built with an internal rip line designed to rip a hole in the side of the balloon for termination of the flight. A special structure was built into the top of the balloon for attaching the top payload. Two poppet valves incorporated into this mounting structure are commanded to open and release helium from the balloon at the end of the flight. The poppet valves act as a backup to the rip line.

Trying to inflate and launch a balloon with a sizeable weight attached to its top is like trying to balance a glass of wine on the horn of a twitchy rhinoceros. A tow balloon tied to the top payload was used during the inflation and launch phases to add stability and keep it on top. This smaller balloon, about 31,000 ft³, is designed to lift about 160 lb (73 kg). The tow balloon was cut loose from the top payload after launch as soon as the main balloon stabilized and the launch-induced oscillations damped out.

3.2 TOP PAYLOAD

The top payload consists of the tracker, solar panel, voltage reference box, multiplexer, data encoder, single-frame movie camera, clock, descent parachute, battery power supply for the tracker and data encoder, relay box, and tracking beacon. All these items were mounted to the aluminum hoop assembly shown in Figure 3. The hoop assembly, with appropriately placed Styrofoam crush pads, served the following functions:

- (1) Permitted the top-mounted payload to "float" on top of the balloon and minimized billowing of balloon material around the top payload.
- (2) Served as the mounting surface for the balloon's top-end fitting.
- (3) Provided a convenient point for attaching the tow balloon and the descent parachute.
- (4) Acted as a shock damper to protect and minimize damage to the top payload at touchdown.

The complete apex-mounted hoop assembly, as flown, weighed approximately 110 lb (50 kg) and descended as a unit by parachute at flight termination.

The sun tracker, shown in Figure 3, is capable of orienting the solar panel toward the sun, compensating for the motion of the balloon by using two-axis tracking in both azimuth and elevation. The tracker has the capability to maintain its lock onto the sun to within ± 1 deg. To verify that the tracker was operating properly, the output of an on-sun indicator was constantly monitored during flight by feeding its output to the multiplexer and entering its signal into the telemetry stream. The on-sun indicator consists of a small, circular solar cell mounted at the bottom of a collimator tube, 7 in. (17.8 cm) long, with an aperture measuring 0.315 in. (0.8 cm) in diameter. The indicator was attached to the solar panel so that it pointed at the sun when the panel was perpendicular to the sun. The output of the on-sun indicator falls off very rapidly as the collimator tube points away from the sun and provides a very sensitive indication of proper tracker operation.

A reflection shield was attached to the panel to prevent any stray reflected light from reaching any of the modules. This shield was made of sheet aluminum and attached to three edges of the solar panel. The shield is the U-shaped, black object shown on the panel in Figure 3.

The solar cell modules were mounted onto the sun tracker platform with an interface of Apiezon H vacuum grease and held in place with four screws. The grease was used to achieve a highly conductive thermal contact between the modules and the panel and to smooth out the temperature distribution over the solar panel as much as possible.

The solar panel temperature was monitored using thermistors. Some of the solar cell modules were constructed with calibrated precision thermistors embedded in the copper substrate directly beneath the solar cell. Four of these modules were mounted on the solar panel at strategic locations so their temperature readings gave an accurate representation of panel temperature. Placement of these modules on the panel is shown in Figure 2.

The pulse code modulation (PCM) data encoder amplified the analog signals from the solar cells, thermistors, on-sun indicator, and reference voltages, then performed an analog-to-digital conversion. The encoder had a programmable control unit that was used to set bit rate, bits per word, parity, analog-to-digital conversion, and format. Two 32-channel multiplexers allow sampling of up to 64 data channels and amplify the low-level signals from the experimental package. The amplifier was designed to process voltage signals at input levels up to 100 mV. The multiplexer stepped through the various channels at a rate of two scans per second, i.e., every data channel is read twice each second.

An ultrawide-angle, single-frame movie camera mounted at the perimeter of the aluminum hoop provided visual documentation of tracker operation. A battery-powered timer activated the shutter at 10-second intervals, so that 50 ft of 8-mm movie film is sufficient to record the entire flight from launch to landing. A windup clock was placed in the camera's field of view for correlation of tracker operation with the telemetered data. The pictures provide a complete record of ascent, tracker operation at float altitude, descent, touchdown, and post-touchdown events.

A tracking or locator beacon was attached to the hoop assembly. This beacon, similar to those used for tracking wild animals in their natural habitat, consists of a low-wattage transmitter which sends short 160 MHz pulses at the rate of about one per second. A hand-held directional antenna and a battery powered receiver are used inside the chase plane and on the ground for locating the transmitter. This beacon has been very useful in locating this very small payload in a very large open range.

3.3 BOTTOM PAYLOAD

The bottom payload was entirely furnished by the NSBF. It consists of a battery power supply, a ballast module for balloon control, and an electronics module known as the consolidated instrument package (CIP).

Power for operating most of the electrical and electronic equipment on the balloon was supplied by a high-capacity complement of lithium batteries. This supply, furnishing 28 Vdc regulated power and 36 Vdc unregulated power, powered all the instruments in the CIP. Several other small battery sources were used at various locations on the balloon for instruments that require small amounts of power. For example, the tracker and data encoder, the tracking beacons, the voltage reference box, and the camera timer all had individual battery power supplies. All batteries were sized to supply power for at least twice the expected duration of a normal flight.

High-altitude balloons tend to lose helium slowly during the course of the flight. As a consequence, a helium balloon will tend to reach float altitude and then begin a slow descent. To counteract this tendency, a ballast system was included as part of the bottom payload. It contained approximately 100 lb (45 kg) of ballast in the form of very fine steel shot. The shot may be released in any desired amount by radio command. By proper use of this system, float altitude may be maintained to within $\pm 2,000$ ft (± 600 m).

The telemetry system was contained in the CIP. A block diagram of the telemetry system is shown in Figure 4. The system sent all data transmissions concerning the flight over a common RF carrier. The CIP also contained a command system for sending commands to the balloon for controlling scientific payloads or for controlling the housekeeping functions on the balloon. Specifically, the CIP contained the following equipment:

- (1) MKS pressure transducers
- (2) Omega receiver
- (3) Subcarrier oscillators, as required
- (4) L-band FM transmitter
- (5) High-frequency tracking beacon transmitter
- (6) Transponder for air traffic control tracking
- (7) PCM command receiver-decoder
- (8) Loran receiver
- (9) GPS receiver

The altitude of the balloon was measured with a capacitance-type electronic transducer, which read pressure within the range of 1,020 to 0.4 mbar (102,000 to 40 N/m²) with an accuracy of 0.05%. The transducer produced a dc level that was encoded as PCM data and decoded at the receiving station into pressure, and then the altitude was calculated from the pressure reading.

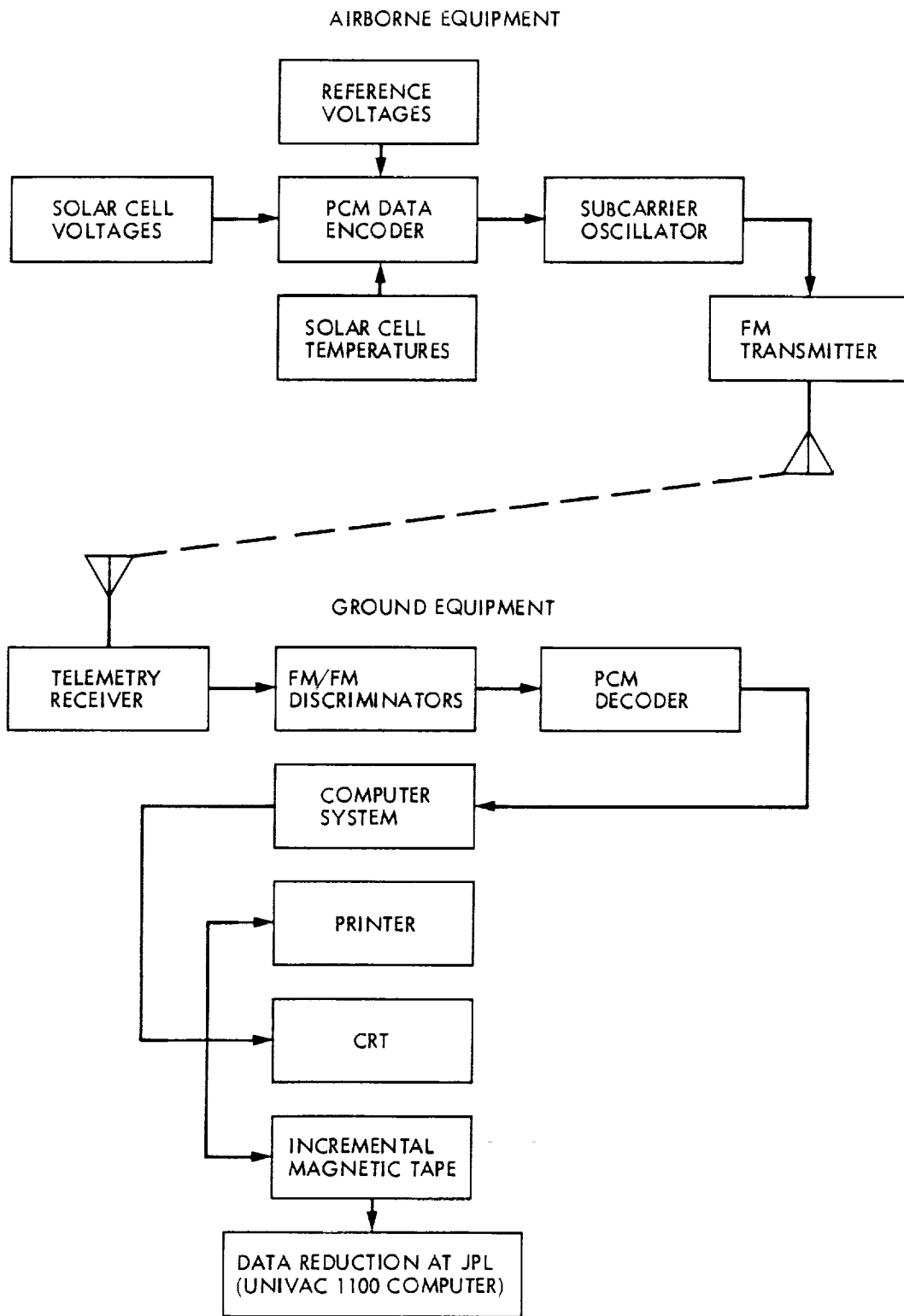


Figure 4. Block Diagram of Balloon Telemetry System

The Omega, Loran, and GPS navigation systems were used for flight tracking. An onboard receiver was used to receive these signals for retransmission to the processor in the ground station. This system can provide position data to an uncertainty of less than 2 mi (3.2 km). The Loran and GPS signals were multiplexed into the telemetry stream and updated every 8 seconds.

As previously mentioned, all the telemetry data were sent to the ground in the form of pulse code modulation. A UHF L-band transmitter in the CIP was used to generate the RF carrier. The L-band carrier was modulated by the pulse code and sent to the receiving station at Palestine.

An aircraft-type transponder was flown so that Air Traffic Control (ATC) could read the balloon's location on their radar systems during the ascent and descent portions of the flight. ATC was helpful in relaying to the recovery aircraft the exact position of the bottom payload during its descent on the parachute.

The purpose of the PCM command system is to send commands to the balloon, e.g., to turn the tracker on or off, terminate the flight, release ballast, etc. It was designed to reject false commands and was highly reliable in operation. The data were encoded on a frequency-shift-keyed audio carrier. This signal was then decoded into data and timing control. Each command consisted of a double transmission of the data word. Both words must be decoded and pass a bit-by-bit comparison before a command can be executed. Commands may be sent to the balloon from either the ground station at Palestine or from the recovery airplane.

The lower payload is suspended from the balloon by an 8.5-m-diameter parachute. The top end of the parachute was fastened to the bottom of the balloon, and the lower payload, which contained the CIP, the battery power supply, and the ballast, was attached to the shroud lines. Appropriate electrical cables and breakaway connectors were rigged in parallel with the mechanical connections. The whole bottom assembly was designed to break away from the balloon and fall to earth while suspended from the parachute at termination of the flight.

4. FLIGHT SEQUENCE

4.1 PRELAUNCH PREPARATIONS

The balloon launchpad at the NSBF is a large circular area, 2,000 ft (600 m) in diameter. In the center of this

large circle is another circular area, solidly paved, measuring 1,000 ft (300 m) in diameter. Grass is planted in the area between the two circles, and a paved road surrounds the larger circle. Paved radials extend from the perimeter road toward the launchpad.

When all prelaunch preparations had been completed and the staff meteorologist had predicted favorable weather and winds at Palestine and for some 300 mi (480 km) downrange, the equipment was taken to the launch site. The main balloon, protected by a plastic sheath, was laid out full-length on the circular paved area. It was aligned with the direction of the wind, with the top of the balloon upwind. The top end of the balloon was passed under, behind, and over the top of a large, smooth, horizontal spool mounted on the front end of the spool vehicle. One end of this launching spool was hinged to the spool vehicle. The other end of the spool had a latch that could be released by a trigger mechanism. After the balloon was passed over the spool, the spool was pushed back to engage the latch so that the spool trapped the balloon. The top 10 m or so of the balloon was pulled forward from the spool, allowing the top payload to rest on the ground. It is this top 10 m of balloon that later receives the helium gas during inflation. The helium forms a kind of bubble in the part of the balloon above the launching spool. After the launching spool was latched, final preparations of the top payload began. The tow balloon was attached to the hoop with nylon lines, the clock was wound, the camera was energized, and a final checkout of the tracker and data encoder was performed.

The launch sequence began by inflating the tow balloon with helium. The main balloon was then inflated by passing a predetermined volume of helium through two long fill-tubes and into the balloon. Figure 5 shows the configuration of the flight train at this stage of preparation. The balloon was launched by triggering the latch on the launching spool. When the latch was released, a stout spring caused the free end of the spool to fly forward, rotating about the hinge, which released the balloon. As the balloon rose, the launch vehicle at the lower end of the balloon began to move forward (downwind). After the driver of the launch vehicle had positioned the vehicle directly below the balloon and had his vehicle going along at the same speed as the balloon, he released the latch on the pin and the lower payload was released. Figure 6 shows the balloon system and the launch vehicle a few seconds after release of the launching spool just as the downwind launch vehicle began to move. As soon as the main balloon quit oscillating, a signal was sent from the launchpad, which

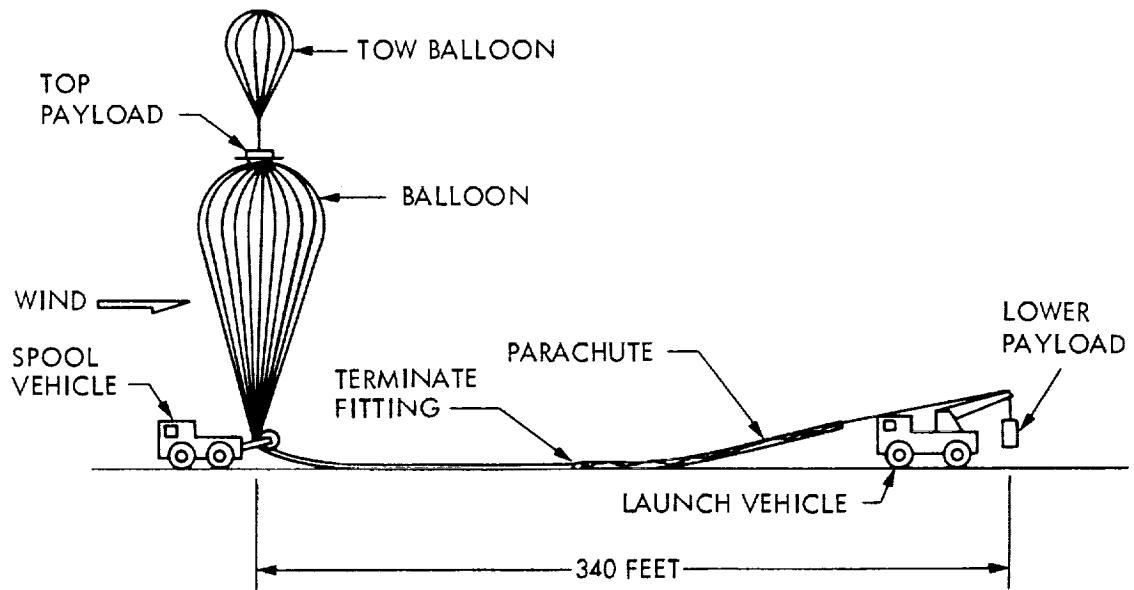


Figure 5. Flight Train Configuration

ORIGINAL PAGE
BLACK AND WHITE PHOTOGRAPH

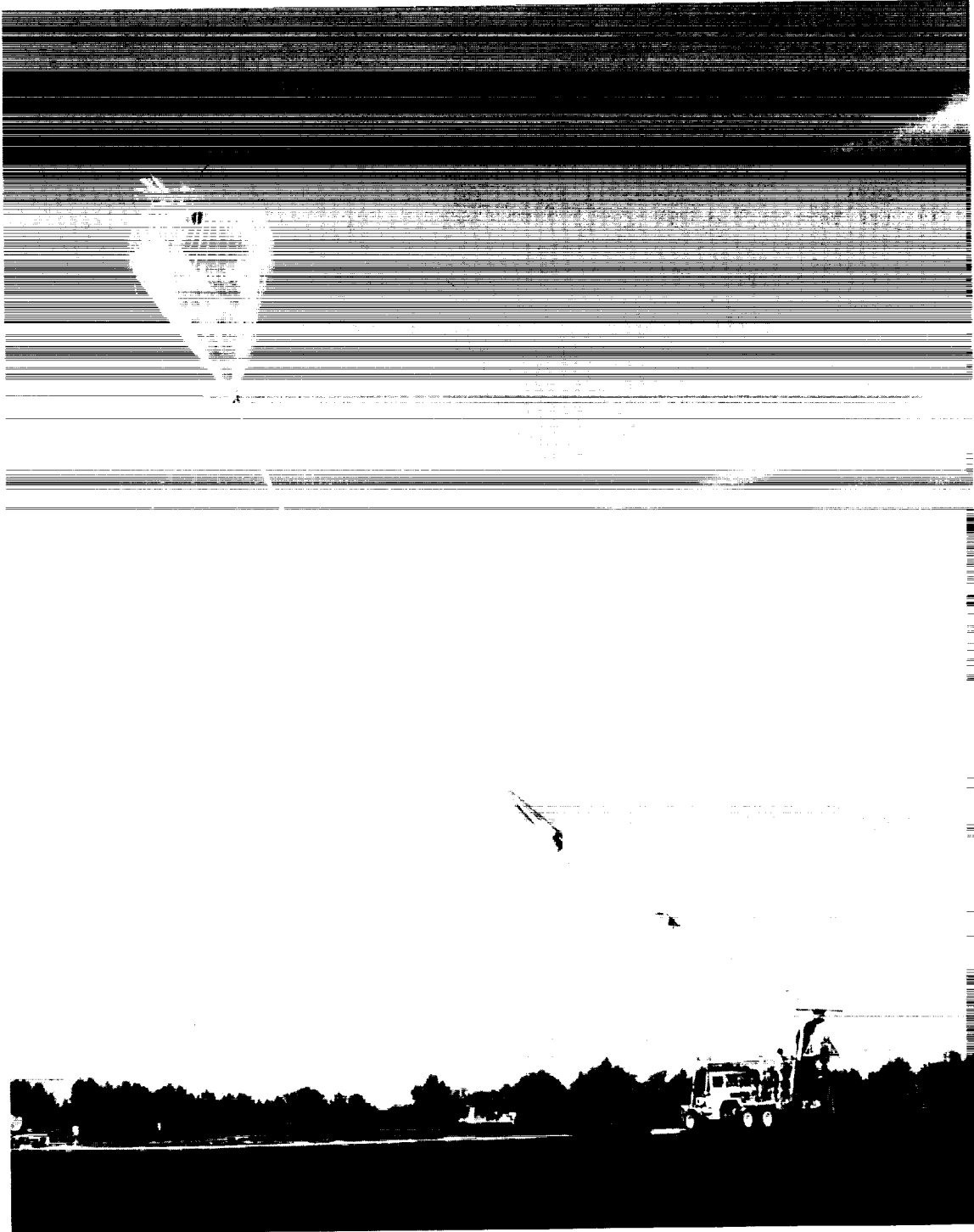


Figure 6. Balloon Launch

triggered an explosive charge. This released the tow balloon, and the launch sequence was complete.

4.2 FLIGHT

The balloon ascended at a rate of approximately 1,000 ft/min (5.0 m/s) and reached float altitude after approximately 2 hours. During the ascent, the flight controller at Palestine maintained a constant contact with ATC. Data from the onboard navigational system were continuously given to ATC so that air traffic in the area could be vectored around the balloon.

After the balloon had been launched, solar cell voltages interspersed with reference calibration voltages and thermistor voltages were fed into the telemetry system. These voltages were converted to PCM and were transmitted to the NSBF ground station along with the navigational, altitude, and other information from the CIP. At the ground station, they were decoded, recorded, and displayed in real time for monitoring of the flight. The balloon reached float altitude at 1546 GMT, which was approximately 3 hours before solar noon. The tracker was turned on by telemetry command a few minutes after reaching float altitude. Tracker operation was monitored by observing the telemetered values for voltage of the battery supply driving the tracker motors, the output of the on-sun indicator, and the outputs of about half the solar cell modules. Data were recorded from time of launch at 1356 GMT through 1906 GMT, when the flight was terminated. Solar noon occurred at approximately 1842 GMT for this flight.

4.3 FLIGHT TERMINATION

Approximately 2 hours after the balloon reached float altitude, the recovery airplane took off from Palestine with the recovery crew aboard. This airplane was equipped with a radio system that allowed the crew to maintain constant communication with the balloon base either by direct transmission or by radio relay from the balloon. The airplane also had a full command system so that it could send commands to the balloon. During the summer months, the winds at altitudes above 80,000 ft (24 km) blow from east to west at speeds of about 50 knots (25 m/sec), so the airplane had to fly about 300 mi (500 km) west of Palestine to be in position for recovery. The pilot could fly directly toward the balloon at any time by flying toward the telemetered location of the balloon. This position information was generated by the Loran and GPS systems on the balloon, telemetered to the Balloon Base at Palestine,

and relayed from there to the airplane. The pilot of the recovery airplane was responsible for termination of the flight. Before leaving Palestine, the pilot had been provided with a set of descent vectors by the staff meteorologist. The descent vectors are estimates of the trajectories that the payloads should follow as they descend by parachute. Upon receiving word from Palestine that the experimenter had all the data he needed, the pilot flew under the balloon and established its position accurately by visual observation. Using the descent vectors, he then plotted where the payloads should come down. He also established contact with ATC. When ATC advised that the descending payloads would not endanger air traffic, and when the descent vector plots showed that the payloads would not come down in an inhabited area, the pilot sent the commands to the balloon for termination of the flight.

The termination sequence consisted of first sending a command that disconnected power from the tracker and data encoder. Next a command was sent that cut the electrical cable running from the bottom payload to the top payload. This command simultaneously cut the cables holding the top payload onto the top of the balloon and opened the poppet valves on the top of the balloon. A second command released the bottom parachute from the balloon, which allowed the bottom payload to fall away and caused the balloon to become top-heavy. As the bottom payload fell, a ripcord attached to the top of the parachute opened a large section in the balloon. The balloon collapsed, the top payload fell off the balloon, its parachute opened, and all three objects began their descent.

Approximately 1 hour is required for the two parachutes and the balloon to fall from float altitude at the descent rate of roughly 1,250 ft/min (6.4 m/s). During this time, the pilot monitored the position of balloon and the bottom payload by visual reference. He also monitored the altitude information from the pressure transducer and relayed this information to ATC. After reaching the ground, all three items had to be found. The beacons on the top and bottom payloads usually aid in locating them rather quickly. Search patterns centered on the impact zones calculated from the descent vectors were flown as necessary. Once the impact locations were established from the air, the ground recovery crew was directed into the proper areas to recover the payloads.

Figure 7 is the flight profile for the 1991 balloon flight (No. 1504P in the nomenclature of the NSBF). The plot shows altitude vs time from the time of launch until touchdown. The points are plotted at approximately 10-min

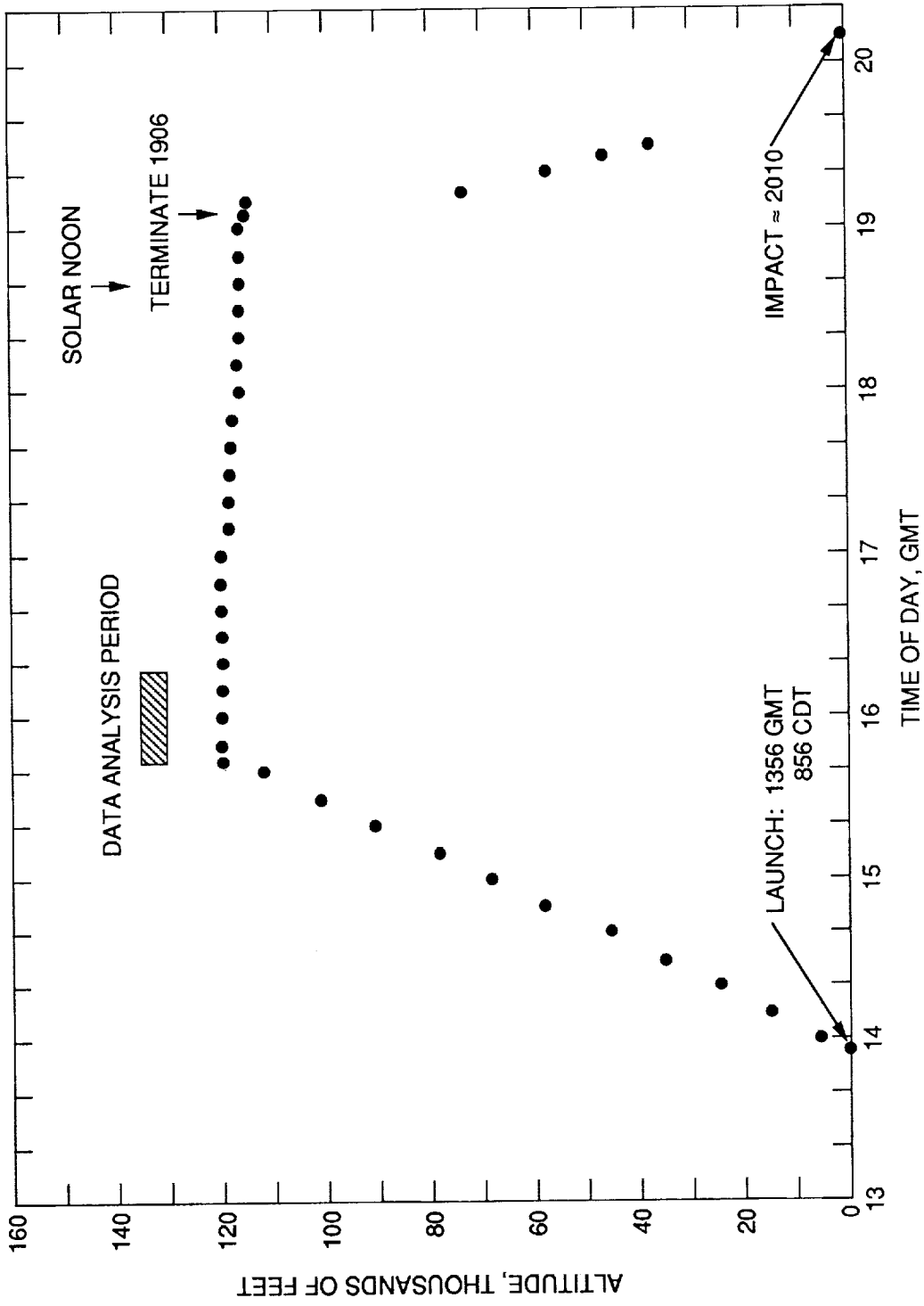


Figure 7. 1991 Balloon Launch Flight Profile

time intervals. The touchdown site was near San Angelo, Texas, approximately 273 mi (439 km) from the launch site. The total flight duration from launch until the terminate command was sent was ≈ 5 hours. The period of time during which computer analysis of the flight data occurred is also shown on the Figure. Data later in the flight were not usable because the tracker developed a mechanical malfunction.

5. DATA ANALYSIS

The computer analysis was performed at JPL by using the Univac 1100 computer. The program read the raw data from the magnetic tape produced during the flight, then corrected the cell data for temperature and sun-earth distance according to the formula:

$$V_{28,1} = V_{T,R}(R^2) - A(T - 28)$$

where

- $V_{T,R}$ = measured module output voltage at temperature T and distance R.
- R = sun-earth distance in astronomical units (AU).
- A = module output temperature coefficient.
- T = module temperature in degrees C.

The remainder of this section describes the details of performing the above corrections and computing calibration values for the cells.

5.1 COMPUTER ANALYSIS

The computer program read data from the magnetic tape one record at a time. Each record contained 16 scans of data plus a ground frame. Each scan of data consisted of two synch words followed by a reading of each of the 64 data channels. The ground frame contained the date and time of the scan followed by the latitude, longitude, and pressure, as measured by instruments on the balloon. The program first checked the ground frame to see whether the record fell within the allowed data analysis time. (The allowed data analysis time window is an input to the program set by the parameters MINTIM and MAXTIM.) The computer rejected the entire frame if the time of the current record fell outside the time window or if it could not read the time properly. The computer read records within the time window until it had accumulated 200 scans. Each set of 200 scans is called a pass. At this point, the data were in pulse code modulation (PCM) counts. The PCM data for each channel were averaged, then a screening

procedure was used to reject scans containing questionable data. For example, scans were rejected if the on-sun indicator was lower than a threshold value (input parameter OSMIN). Scans were also rejected if the PCM count for a data channel was not within the allowable PCM count range, if there was too large a count deviation on any channel from one scan to the next, or if there was an unrecoverable problem in reading the tape.

The PCM data were next converted to engineering units. The program has a provision for doing this in any one of four different ways. The simplest and most commonly used method will be described here. During the calibration of the telemetry system, the output of the telemetry system vs the input from the voltage reference box was recorded to produce a table of mV input vs PCM count output. Similarly for the thermistor channels, a series of resistors was connected one by one across a thermistor channel, and the resulting PCM count for that channel was recorded. Since the temperature corresponding to each resistance value was known, the construction of a PCM count vs temperature table was possible. This procedure was repeated for all thermistor channels, and a calibration table was constructed for each thermistor channel. Both calibration tables were input to the computer program. During conversion of solar cell data to mV, the computer performed a linear interpolation in the PCM vs mV table. At the completion of the initial computer analysis run, the output values of each channel corresponding to voltage reference levels were checked. If they held constant during the flight (they normally read constant to within ± 1 PCM count out of 1,000), the use of the simple linear interpolation scheme was continued for the final data analysis. Since the relationship between thermistor resistance and temperature is nonlinear, a third-degree polynomial was used for the interpolation of the temperature values.

At the end of each pass, four averages were computed for each channel: (1) an initial average based on all acceptable scans, (2) a corrected average using all data falling within a specified fractional deviation (input parameter ADEV) of the initial averages, (3) the corrected average multiplied by the square of the earth-sun radius vector (in AU) for the day of the flight (input parameter RV), and (4) a final average with all the above corrections plus a temperature correction to 28°C. This final correction used the values of the temperature coefficients measured in the laboratory (input parameters TPCOEF). This process completes the data analysis for one pass of data. The entire procedure was repeated by returning to the tape-reading

routine and reading another pass (200 scans) of data. The screening and averaging routines were also performed on this pass. This procedure was iterated until 15 passes of data had been analyzed or until MAXTIM was exceeded. This resulted in 3,000 data points for each cell module on the flight.

In addition to the averages taken after each pass, an overall summary matrix was constructed which contained the fully corrected averages for each channel after each pass. A row of entries was added to this matrix after each pass. After all passes had been completed, an overall average and standard deviation were computed for each channel. These overall averages of 3,000 readings are the reported calibration values for the modules.

5.2 CALIBRATION RESULTS

Table 1 reports the calibration values of all the cells calibrated on the 1991 balloon flight corrected to 28°C and to 1 AU. The Table also reports the standard deviation of the 3,000 measurements, the preflight and postflight readings of each module in the X25 simulator, a comparison of the preflight with the postflight simulator readings, and a comparison of the preflight simulator readings with the balloon calibration readings. The Table also reports the temperature coefficients measured for each module in the laboratory.

5.3 DATA REPEATABILITY

Several standard modules have been flown repeatedly over the 29-year period of calibration flights. Module BFS-17A, which had flown on 41 flights, was used to monitor the repeatability of the balloon flight system. However, BFS-17A was one of the modules destroyed in one of the 1990 flights and is no longer available. As discussed in the 1989 report, the calibration values for BFS-17A averaged to a value of 60.180 over its 41 flights, with a standard deviation of 0.278 (0.46%). In addition to giving a measure of the consistency of the year-to-year measurements, BFS-17A also provided insight into the quality of the solar irradiance falling on the solar panel, with regard to uniformity, shadowing, or reflections. This cell had been mounted in various locations on the panel over the years. Nevertheless, its readings were always consistent, which verified that there are no uniformity, shadowing, or reflection problems with the geometry of this system.

We have identified a group of solar cells which will be used as replacements for the function served by BFS-17A. Some cells from this group will be flown every year so that we can continue our year-to-year continuity checks. We chose seven samples from this group for flight in 1991. Four of these cells were Si cells, two of which were flown on the shuttle. The other three are GaAs cells. Data from these cells are presented in Table 2. These measurements and comparisons indicate that the 1991 calibration values are consistent with those of previous years.

6. CONCLUSIONS

The 1991 balloon flight was a success. Twelve cells from previous flights were reflown this year. Of these 12, 7 are Si cells and 5 are GaAs cells. Considering only the Si cells belonging to JPL, the maximum deviation of the 1991 data from the average data was -0.29%. For the JPL GaAs cells, the maximum deviation of the 1991 data from the average was 0.63%. These results and comparisons are similar to those achieved in previous flights, and we believe that the calibration values obtained from the 1991 flight can be used with a high degree of confidence.

7. REFERENCE

B. E. Anspaugh, R. G. Downing, and L. B. Sidwell, *Solar Cell Calibration Facility Validation of Balloon Flight Data: A Comparison of Shuttle and Balloon Flight Results*, JPL Publication 85-78, Jet Propulsion Laboratory, Pasadena, California, October 15, 1985.

Table 1. 1991 Balloon Flight 8/1/91 119,000 ft, RV = 1.0149684, Flight No. 1504P

COMPARISON - SOLAR SIMULATOR & FLIGHT									
MODULE NUMBER	ORG.	TEMP INTENSITY ADJUSTED AVERAGE	STD. DEV.	AMO, SOLAR SIM. 1 AU 28 DEG C.		PRE-FLT. VS. POST-FLT.	FLIGHT VS. PRE-FLT.	TEMP. COEFF. (MV/C)	COMMENTS
				PRE-FLT	POST-FLT	(PERCENT)	(PERCENT)		
91-141	AERO	60.14	.0973	58.61	58.17	-.75	2.39	.0429	GaAs/Ge
91-001	AFPL	84.17	.0855	85.42	85.11	-.36	-1.61	.0441	ASEC BSFR 10 Ohm 8 mil
91-011	AFPL	79.11	.0584	79.81	79.12	-.86	-.96	.0508	ASEC BSR 2 Ohm 8 mil
91-012	AFPL	78.55	.0692	79.00	78.56	-.56	-.66	.0511	ASEC BSR 2 Ohm 8 mil
91-014	AFPL	84.19	.0900	85.27	84.93	-.40	-1.43	.0427	ASEC BSFR 10 Ohm 8 mil
91-015	AFPL	82.48	.0580	85.61	85.46	-.18	-3.73	-.0001	Boeing CIS
91-016	AFPL	60.67	.0846	58.90	58.78	-.20	2.84	.0428	GaAs/Ge
91-017	AFPL	62.28	.1004	60.40	60.30	-.17	2.83	.0491	GaAs/Ge
91-150	ASEC	63.12	.0746	60.09	59.52	-.95	4.97	.0404	GaAs/Ge LMSC 4X4
91-151	ASEC	62.38	.0764	59.38	58.78	-1.01	4.93	.0399	GaAs/Ge LMSC 4X4
91-110	HAC	74.66	.0627	73.88	72.91	-1.31	1.06	.0731	SPL K4 3/4 6X6
STS-010	JPL	74.14	.0601	73.78	74.26	.65	.42	.0435	K6 3/4 10 Ohm 2 mil Refly
STS-025	JPL	74.46	.0518	74.88	74.84	-.05	-.66	.0442	K6 3/4 10 Ohm 2 mil Refly T4
80-004	JPL	77.98	.0763	78.26	77.70	-.72	-.45	.0443	K4 3/4 10 Ohm 10 mil Refly
84-001	JPL	59.57	.0961	57.85	57.60	-.43	2.72	.0494	GaAs Refly
86-023	JPL	59.12	.0730	57.24	57.12	-.21	3.12	.0454	GaAs MANTECH Refly T2
86-024	JPL	58.89	.0735	57.21	56.76	-.79	2.81	.0456	GaAs MANTECH Refly T1
86-025	JPL	87.34	.0707	87.77	87.93	.18	-.59	.0478	ASEC K6 3/4 8 mil Refly T3
90-002	JPL	61.14	.1032	59.59	59.18	-.69	2.40	.0361	ASEC GaAs/Ge Refly
91-002	JPL	78.26	.0602	78.57	78.25	-.41	-.47	.0484	ASEC BSR 2 Ohm 8 mil
91-003	JPL	83.43	.1232	84.76	84.65	-.13	-1.77	.0444	ASEC BSFR 10 Ohm 8 mil
91-004	JPL	83.92	.1019	85.15	84.84	-.36	-1.62	.0425	ASEC BSFR 10 Ohm 8 mil
91-005	JPL	82.46	.0710	85.32	85.43	.13	-3.40	-.0021	Boeing CIS
91-013	JPL	78.49	.0554	78.93	78.62	-.39	-.61	.0490	ASEC BSR 2 Ohm 8 mil
83-101	RMC	60.60	.0894	59.00	58.31	-1.17	2.51	.0417	GaAs Refly
83-103	RMC	61.06	.0930	59.48	58.77	-1.19	2.49	.0445	GaAs Refly
83-105	RMC	79.60	.0530	79.45	79.27	-.23	.20	.0381	Si 2 mil Refly
83-106	RMC	79.64	.0680	79.64	79.71	.09	-.02	.0404	Si 2 mil Refly
91-120	RMC	80.39	.0614	80.69	80.30	-.48	-.40	.0444	Sharp BSFR 10 Ohm 2 mil
91-121	RMC	81.09	.0863	80.84	80.85	.01	.22	.0457	Sharp BSFR 10 Ohm 2 mil
91-122	RMC	81.35	.0689	81.37	80.94	-.53	-.03	.0436	Sharp BSF 10 Ohm 8 mil
91-123	RMC	81.25	.0660	81.47	81.09	-.47	-.32	.0447	Sharp BSF 10 Ohm 8 mil
91-170	SPL	78.97	.0818	79.34	78.79	-.69	-.58	.0459	BSR 2 Ohm
91-172	SPL	62.79	.0948	61.13	61.03	-.16	2.47	.0462	GaAs/Ge
91-175A	SPL	66.95	.0678	64.49	63.08	-2.19	3.91	.0113	GaInP2/GaAs
91-175B	SPL	72.68	.1680	71.55	71.17	-.53	1.25	.0661	GaInP2/GaAs
91-177A	SPL	52.09	.1781	56.41	56.71	.53	-7.19	-.0090	3 mil K7/GaAs FILTER
91-177B	SPL	55.09	.1474	59.48	59.83	.59	-7.00	-.0214	4 mil K7/GaAs FILTER
91-160	SSL	81.99	.0734	82.13	81.76	-.45	-.23	.0460	Sharp BSR 2 Ohm 8 mil
91-162	SSL	82.80	.0715	83.30	82.96	-.41	-.68	.0477	Sharp BSR 10 Ohm 8 mil
91-130	TRW	78.58	.0540	79.12	79.00	-.15	-.77	.0407	BSFR 3 mil Thin
0 mV		.00	.0000	.00	.00	.00	.00	.0000	
50 mV		49.97	.0410	.00	.00	.00	.00	.0000	
80 mV		79.99	.0435	.00	.00	.00	.00	.0000	
100 mV		99.83	.0540	.00	.00	.00	.00	.0000	

Table 2. Repeatability of Eight Standard Solar Cell Modules Over an 11-year Period

Flight Date	80-004 K 4 3/4 BSR	84-001 GaAs LPE	STS-010 K 6 3/4 BSFR	STS-025 K 6 3/4 BSFR	86-023 Mantech GaAs	86-024 Mantech GaAs	86-025 BSFR K 6 3/4	90-002 GaAs/Ge
7/24/80	78.06							
7/21/82	78.05							
7/19/84		59.99						
8/84 Shuttle			75.01	75.31				
7/12/85			74.61	75.04				
7/15/86					58.46	58.44	87.71	
8/23/87		59.63			59.47	59.59	87.99	
8/7/88		58.68	73.28	73.87	58.26	58.36	87.00	
8/9/89					58.30			
9/6/90	78.33			74.71	58.89	58.84	87.77	61.12
8/1/91	77.98	59.57	74.14	74.46	59.12	58.89	87.34	61.14
Average	78.105	59.468	74.260	74.678	58.750	58.824	87.562	61.130
Std. Deviation	0.154	0.557	0.744	0.555	0.490	0.488	0.392	0.014
Max. Deviation	0.225	0.788	0.980	0.808	0.720	0.766	0.562	0.010

